

Modelling the microclimate of a Saxonian terraced vineyard with ENVI-met

Modellierung des Mikroklimas eines sächsischen Terrassenweinbergs mit ENVI-met

Adrien Noirault, Roland Achtziger, Elke Richert, Valeri Goldberg, Barbara Köstner

Summary: Saxony is one of the northernmost winegrowing regions in Europe. Most of its vineyards are located on steep slopes in the Elbe valley. Therefore, microclimatic conditions in the vineyards are of major importance for viticulture. In this study the applicability of the computing program ENVI-met in simulating the microclimate of vineyards was tested. Initially designed for urban areas, here we used this software to simulate the microclimate for a typical Saxonian vineyard. For this purpose, a 3D model of the vineyard was created and all input parameters needed for the simulations concerning climate, soil, vegetation etc. were implemented. In this paper a sensitivity analysis and first results on daily courses and the spatial distribution of several climatic and physiological variables are presented. The daily courses of climatic and physiological parameters obtained by the simulations for a typical summer day (18th July 2019) were consistent with theoretical assumptions and literature. The model application to variations in input parameters or changes in vineyard structure offers new opportunities to estimate the effects of specific management practices on microclimate and the performance of vines in vineyards.

Keywords: Weinberge, Mikroklima, Weinbau, Modellierung, Sachsen / vineyards, microclimate, viticulture, modelling, Saxony

1. Introduction

Understanding the effect of vineyard structure, composition and agricultural practices on microclimate could help winegrowers in their management choices. This becomes especially important for adapting to climate change impact. Up to now, many studies have shown the impact of management practices on vineyard performance. For instance, ground and canopy management largely influences soil properties and water status (Celette et al. 2008; Steenwerth & Belina 2008; Sharifi et al. 2018; Vukicevich et al. 2018; Guzmán et al. 2019; Gattulo et al. 2020), another example is row orientation which modifies wind direction and speed but also humidity and vine transpiration (Bodor et al. 2014; Hunter et al. 2016, 2020). Using the ENVI-met software to model microclimatic situations in vineyards, we investigated several management scenarios to analyse their effects on vineyard microclimate and vine performance (e.g., physiological status).

ENVI-met is a computing program initially designed to simulate microclimate in urban environments (Bruse & Fleer 1998). It has been created for architects and urban management to investigate the effect of building materials and structures on urban microclimate. In particular it can help in preventing the building up or reinforcement of urban heat islands (Deilami et al. 2018). Also, as viticulture is highly dependent on the local climate (temperature, solar radiation, humidity) which greatly influences wine production, quality and taste (Marais et al 1999, 2001; Lee et al. 2007), we decided to use the software to model microclimate in the context of a vineyard. In particular, being able to understand and model the effect of vineyard management on the microclimate and the performance of vineyard could be very useful in the perspective of climate change and temperature rise (Hannah et al 2013; Fraga et al 2015; Aragón-Durand et al. 2018; Santos et al. 2020).

Wine growing regions are not equally distributed all over the world and their climatic environment is not the same worldwide (Jackson 2014). In this study we focussed on the wine growing region of Saxony. This is one of the northernmost wine-growing regions in Europe with only 500 ha of vineyards (DWI 2020; LfULG 2020) located along the river Elbe in the South and North of Dresden between Pirna and Diesbar-Seußlitz. As most of the Saxonian winegrowers work part-time or as hobbyists, this region only counts about 40 full-time wineries (LfULG 2020). Many of the steep vineyards have terraces with dry stone walls to interrupt the slope and make the vineyards cultivable (Weinbauverband Sachsen 2016). Most of them have a south-east to south-west aspect to take advantage of the higher temperatures and the longer exposition to sunlight.

Using the free version of the software ENVI-met 4.0 (Huttner & Bruse 2009) we simulated the microclimate in a typical Saxonian vineyard with all its elements (ground cover, slopes, walls, etc.) to estimate the applicability of this software to vineyards. Here we present the basic results obtained from a sensitivity analysis and the implementation of a model vineyard.

2. Study area and Materials

2.1 Study area: the Friedstein vineyard

The vineyard we used as basis for modelling was the smaller section of the Friedstein vineyard (named Friedstein I, see Fig. 1) located in Radebeul. It has been reconstructed and recultivated by Martin Schwarz in 2009 after being abandoned for about 80 years (Martin Schwarz, pers. comm.). This vineyard consists of three main terraces with several smaller terraces and three walls (Fig. 1). It well represents traditional vineyards from this region. Moreover, it is relatively new and regular which is an advantage for the implementing in ENVI-met as the program only allows basic design and parallel structures. The walls in the vineyards are rather parallel, quite new and therefore have more or less the same color. Due to these properties comparable to urban green areas, coupled with available information on geology, soil and climate, we chose this vineyard for a first application of ENVI-met to vineyards.

2.2 Climate data

All climate data are from the German Climate Data Centre (DWD 2020). In particular we used data from the Dresden-Hosterwitz meteorological station, a station in the south-east of Dresden in the Elbe valley and in the vicinity to vineyards. We downloaded hourly and daily air temperature, relative humidity and we calculated the daily mean for wind speed and direction at 10 m height. For soil data we also used the German Climate Data Centre (DWD 2020) to get values for soil temperatures and soil moisture at 10 cm, 50 cm and 1 m depth. We decided to model a typical day of July (18th of July 2019) with an average daily temperature of 22.4°C (Fig. 2). This day has been chosen as it happens in the middle of the reproductive period (Jackson 2014), between flowering and veraison. All the results will be shown in degree Celsius.

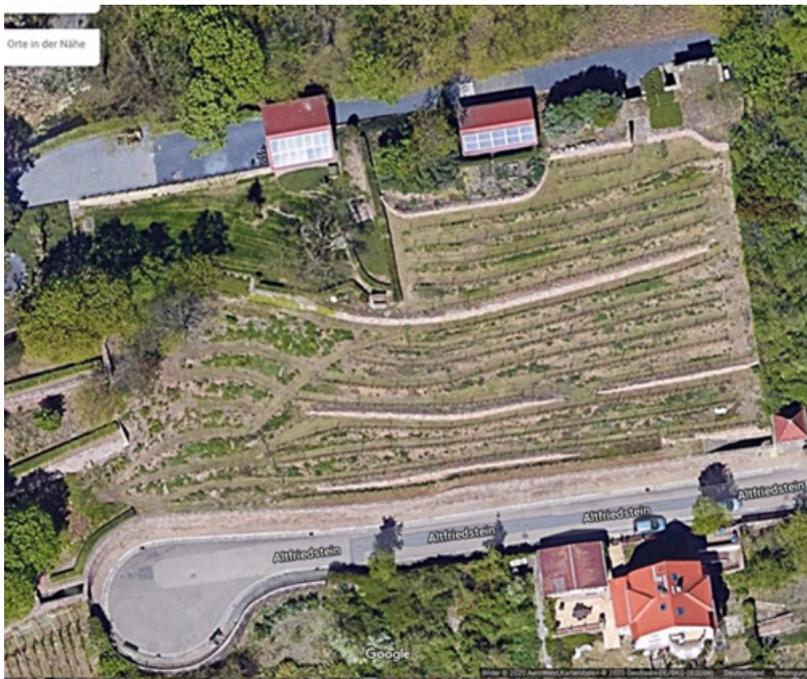


Fig. 1: Aerial photo of the modelled part of the model vineyard Friedstein I: 51°06'55.6"N 13°37'39.7"E (Radebeul, Elbe valley, Saxony) (Source: Google Earth Geobasis-BE/BKG ©2009).

Abb. 1: Luftaufnahme des modellierten Weinbergs Friedstein I: 51°06'55.6"N 13°37'39.7"E (Radebeul, Elbtal, Sachsen) (Quelle: Google Earth Geobasis-BE/BKG ©2009).

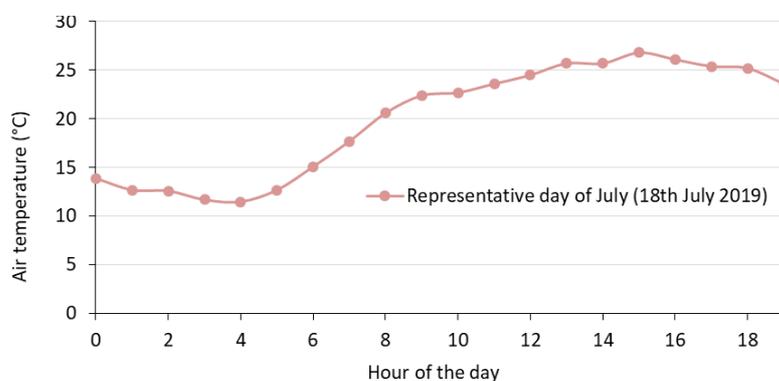


Fig. 2: Daily course of air temperature for the modelled typical day in July (18th of July, 2019) (data source: DWD, meteorological station Dresden-Hosterwitz).

Abb. 2: Tagesverlauf der Lufttemperatur für den modellierten typischen Julitag (18. Juli 2019) (Datenquelle: DWD, Wetterstation Dresden-Hosterwitz).

2.3 ENVI-met software

To implement the 3D model of the vineyard we used the SPACES software which is part of ENVI-met. This feature allows the creation of multiple objects such as vegetation, buildings or walls and it permits the implementation of a digital elevation model. For model computation we used ENVI-met V4.0 Preview II (Huttner & Bruse 2009). The average computation time was about 12 hours. All analyses were made using the LEONARDO 3.0 software from ENVI-met. The workflow used for modelling is shown in Fig. 3 and details about database implementation and area input file are available in chapter 3.

2.4 Evaluation of model results

The first category of variables studied were climate variables such as wind speed, air temperature and relative humidity, solar radiation balance (direct radiation + diffuse radiation – reflected radiation), soil moisture and soil latent heat flux. Vapor pressure deficit (VPD) was calculated using the Tetens equation (Monteith & Unsworth 2013) that is highly precise for temperature between 0°C and 50°C (Lide 2005). The second category were variables representing plant (here: grapevine) conditions or physiology. First, vine leaf temperature which is an indicator of plant water stress (Dhillon et al. 2014). Second, stomatal conductance (or resistance) which is also an important physiological variable that measures the rate of passage of carbon dioxide (CO₂) entering, or water vapor exiting through the stomata of a leaf. It is a function of stomatal density, stomatal aperture, and stomatal size (Zeiger et al. 1987) and changes in maximum values can also be used as an indicator of plant water deficit (Oosterhuis & Walker 1987). Third, CO₂ flux and vapor flux were simulated to analyse photosynthesis and transpiration. Water use efficiency (WUE), which is defined as the amount of carbon assimilated per unit of water used, was also calculated with these variables.

Table 1 shows the typical or optimal range for grapevine obtained from literature for each of the variables that have been modelled. All the variables described above were analysed with time series from 0.00 am to 19.00 pm.

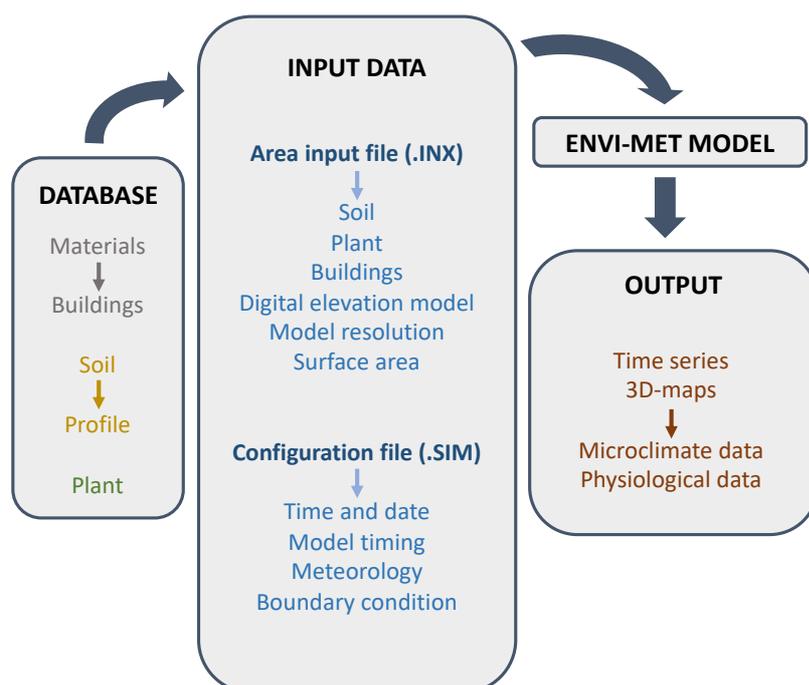


Fig. 3: Workflow in ENVI-met: The first step is to implement the ENVI-met database with parameters of the surface structures (material), soil and plants. Then, an area input file (.INX) is needed with all the elements to design the 3D model of the studied area. A configuration file (.SIM) is also created with the initial data for meteorology and model timing. Then the simulations can be run with ENVI-met. Finally, the outputs can be shown as time series or 3D-maps for both climate and physiological data.

Abb. 3: Arbeitsablauf in ENVI-met: Im ersten Schritt werden die Parameter für die Oberflächenstruktur (Material), den Boden und die Pflanzen in die ENVI-met-Datenbank eingetragen. Anschließend wird ein area input file (.INX) mit allen Strukturelementen benötigt, um ein 3D-Modell der Untersuchungsfläche zu erstellen. Zudem wird ein configuration file (.SIM) mit den Eingangsdaten für Meteorologie, Zeitpunkt und Daten erstellt. Dann können die Simulationen in ENVI-met gestartet werden. Die Ergebnisse können in Form von Zeitreihen oder 3D-Karten bzgl. der mikroklimatischen und physiologischen Parameter ausgegeben werden.

Table 1: Typical values for several parameters and variables. The optimal range refers to the values maximizing grapevine growth and photosynthesis, the common range refers to observed values in vineyards.

Tabelle 1: Typische Werte für verschiedene Parameter und Variablen. Der optimale Bereich bezieht sich auf geeignete Werte für eine Maximierung von Wachstum und Photosynthese der Weinreben; der allgemeine Bereich bezieht sich auf üblicherweise gemessene Werte in Weinbergen.

Variable	Optimal range	Reference
Leaf temperature	25 to 30°C	Greer (2012)
Water use efficiency	2 to 6 gCO ₂ /L	Flexas et al. (2010)
Vapor pressure deficit	0.8 to 1.2 kPa	Koverda (2020)
Stomatal conductance	165 to 665 mmol/(m ² *s)	Zeiger et al. (1987)
Variable	Common range	
CO ₂ flux	220 to 400 mg/(m ² *s)	Greer (2012)
Transpiration	20 to 100 mg/(m ² *s)	Greer (2012)
Wind speed	1 to 6 m/s	Piennar (2005)

Table 2 and Fig. 3 show at which height and for which area we analysed the data for each variable.

Table 2: Height of observation layer and observed area for each variable studied.

Tabelle 2: Höhe der betrachteten Ebene und betrachtete Fläche.

Studied variable	Height of observation	Observed area
Stomatal conductance	1.5 m	Upper height of grapevines
Leaf temperature	1.5 m	Upper height of grapevines
Vapor flux	1.5 m	Upper height of grapevines
CO ₂ flux	1.5 m	Upper height of grapevines
Wind speed	From ground to 15 m	See Fig. 6b
Relative air humidity	0.5 m	See Fig. 6a
Soil moisture	0.005 m	See Fig. 6a
Air temperature	1.5 m (grapevine height)	See Fig. 6a

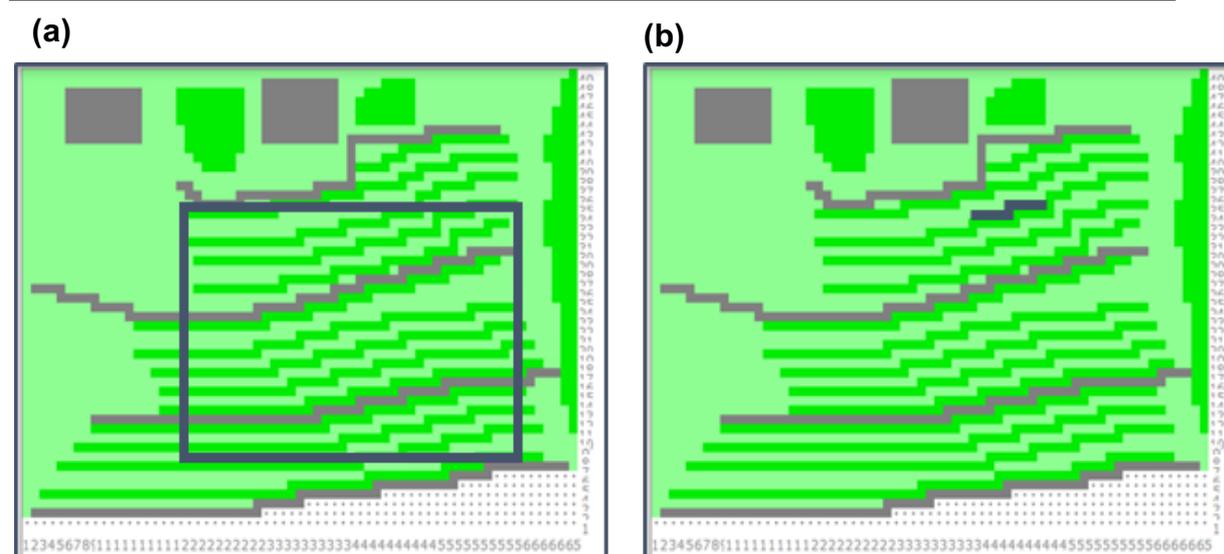


Fig. 4: Area used for the analysis of (a) air temperature, relative air humidity, soil moisture and soil latent heat flux, (b) wind speed.

Abb. 4: Genutzte Bereiche für die Analyse von (a) Lufttemperatur, relative Luftfeuchtigkeit, Bodenfeuchte und latenter Wärmefluss vom Boden, (b) Windgeschwindigkeit.

3. Methods: Implementation of ENVI-met for the model vineyard Friedstein I

3.1 Vegetation types and characteristics

First of all, we defined grapevine rows by parameterizing grapevine plants in the ENVI-met database. For the growth height, based on field observations, we chose 1.5 m as an average value and we used 2.0 m for the root zone depth. Leaf albedo was set at 0.28 as found by Pieri & Gaudillère (2003). Additionally, ENVI-met needs a leaf area density (LAD) profile, i.e. it separates grapevine in 10 vertical layers with a LAD value for each layer. Leaf area density (LAD, m^2/m^3) is defined as the one-sided area of leaves per unit volume (Jonckheere et al. 2004). To estimate the mean LAD we divided the leaf area index of $1.50 \text{ m}^2/\text{m}^2$ (from Fuentes et al. 2014) by the average growth height. Then we estimated the proportion of maximum leaf area available for each layer (100 % for the layer with the most important leaf area) and assigned the LAD value for each layer according to its contribution to the total leaf area. The results for grapevine are shown in Table 3. Layer 9 and 10 without LAD represent the leafless sections in the lower part of the trunk above the ground.

In order to test the effect of ground cover on vineyard microclimate, we implemented ground vegetation parameters in the ENVI-met database. In a previous study, Benyr (2018, unpubl.) provided a habitat and vegetation map for the Friedstein vineyard. Based on this and other data on groundcover vegetation of Saxonian vineyards, we defined several vegetation types according to their phenological and structural characteristics. For the modelling we used a type of low-growing plant species (LG) and a type with high growing species (HG) (Table 4): Whereas the LG type was mainly composed of perennial species well adapted to dry, warm and nutrient poor conditions such as Crassulaceae (e.g. *Sedum acre*) or species with rosettes such as *Pilosella officinarum*, the HG type was dominated by several perennial herbs and grasses typical for mesophilic sites. For the growth height of the two vegetation types we referred to data of Benyr (2018, unpubl.), Weber (1997, unpubl.), Zöphel & Mahn (2000), and own field measurements. For albedo the base value already implemented for grass in ENVI-met (0.20) was kept. As there were no data for LAD values of grassland or ground vegetation, we had to use estimated values based on field data from Benyr (2018, unpubl.) for vegetation cover (%) and the sum of abundances of all species per plot. Table 4 shows that, for both vegetation types, the sum of abundances is only slightly higher than the vegetation cover. This indicates that there was very low spatial overlap of the plant parts in the stands. Nevertheless, the vegetation cover probably underestimates the real LAI, specifically for the HG type with its numerous species of different growth forms. The large differences in LAD are resulting from the different growth heights of the two vegetation types (Table 4). Additionally, we tested the effect of total ground cover (FC: full cover) vs. cover only in interrows (PC: partial cover) vs. bare soil (BS).

Table 3: Values used for the calculation of grapevine LAI (leaf area index) and LAD (leaf area density) for each layer.

Tabelle 3: Verwendete Werte zur Bestimmung des LAI (Blattflächenindex) und des LAD der Weinreben (Blattflächendichte) pro Layer.

Layer	Layer's height (m)	Percentage of maximum leaf area available in layer i	Percentage of leaf area available for layer i	LAI for layer i (m^2/m^2)	LAD on volume i (m^2/m^3)
1	0.15	90%	15%	0.23	1.50
2	0.15	100%	17%	0.25	1.67
3	0.15	100%	17%	0.25	1.67
4	0.15	100%	17%	0.25	1.67
5	0.15	90%	15%	0.23	1.50
6	0.15	70%	12%	0.18	1.17
7	0.15	40%	7%	0.10	0.67
8	0.15	10%	2%	0.03	0.17
9	0.15	0%	0%	0.00	0.00
10	0.15	0%	0%	0.00	0.00

Table 4: Characterization of the vegetation types used for the modelling based on Benyr (2018 unpubl.) and own field observations.

Tabelle 4: Charakterisierung der für die Modellierung verwendeten Vegetationstypen basierend auf Benyr (2018 unpubl.) und eigenen Beobachtungen.

Vegetation types	Low-growing species type (LG)	High-growing species type (HG)
		
Parameters		
Site conditions	warm, dry, nutrient poor and acidic	warm, mesophilic (medium soil moisture, nutrient content and acidity)
Characteristic species (examples)	<i>Pilosella officinarum</i> <i>Vicia angustifolia</i> <i>Potentilla argentea</i> <i>Poa angustifolia</i> <i>Sedum</i> spp.	<i>Echium vulgare</i> <i>Melilotus albus</i> <i>Daucus carota</i> <i>Artemisia vulgare</i> <i>Achillea millefolium</i> <i>Festuca rubra</i>
Species richness	low to medium	high
Dominating species	perennial herbs dominating, only few grasses	perennial herbs and grasses
Mean growth height (cm)	20	50
Mean vegetation cover (%)	80	70
Mean sum of species abundances (%)	90	92
Estimated LAI (m²/m²)	0.8	0.8
Estimated LAD (m²/m³)	3.2	1.12

As a last step in implementing the plant database, we created a “fictive plant” combining grapevine and ground vegetation to model the case in which there is vegetation just below the grapevines (“Unterstockbereich”). We used the height and albedo for grapevine, and we added the LAD of ground vegetation in the corresponding layer(s) (depending on the height of the vegetation type).

3.2 Implementation of soil parameters

To create the soil profile in the database manager, we used data about Saxonian vineyards (LfULG 2017) on soil composition of the upper 2 m. As it was mainly sand with some loam, we defined a mixed soil profile with many sandy layers and some loamy sand layers for the implementation of soil profile parameters in ENVI-met. Furthermore, we implemented the properties of the soil surface as follows: (1) Soil roughness length is equivalent to the distance from maximum height of soil to the level at which the wind speed theoretically becomes zero (American Meteorology Society 2019). It is affected by soil composition and soil management (da Rocha Junior et al. 2016). ENVI-met needs a single average value and we used both literature data (Kwast et al. 2013; Jiang & Weng 2016) and the ENVI-met database to estimate this parameter for our soil (roughness length = 0.020 m). (2) Soil albedo is the proportion of solar radiation reflected from soil surface relative to total incoming solar radiation (Dobos 2011). It depends on many parameters such as composition and tillage (Oguntunde et al. 2006). The vineyards’ soil surfaces (upper 5 cm) are described as rather dark due to the humus contents (LfULG 2017). Thus we decided to use the albedo from a sandy soil with humus from the literature (soil albedo = 0.16, Stoutjesdijk & Barkman 2014). (3) Soil emissivity measures the efficiency in which a surface emits thermal energy. It is defined as the fraction of energy being emitted relative to that emitted by a thermally black surface (Qin & Karnieli 1999). For our model we used an average value (0.93) from the literature (Qin & Karnieli 1999; An et al. 2017).

3.3 Implementation of wall parameters

In ENVI-met there are different ways to implement walls: single walls and buildings. As single walls are only meaningful when located on buildings, we used building elements as walls instead of single walls. A field excursion revealed that walls are mainly built by syenite, which is similar to granite. We defined a new material corresponding to granite in the ENVI-met database and implemented the multiple properties needed (Table 5). Finally, as a wall is on average 1 m thick and as, in ENVI-met, it is composed of three layers, we chose to implement a default thickness of 35 cm for the basic granite material.

Wall albedo varies with the colour of the surface which depends mainly on the age of the wall (see Fig. 5). For example, Synnefa et al. (2009) have shown a difference in solar reflection of about 0.18 between a beige and a dark green asphalt layer. So, we decided to implement a difference of 0.15 in the albedo between new walls (beige, albedo = 0.30) and old walls (brown to black, albedo = 0.15).

3.4 Implementation of the digital elevation model (DEM)

The Friedstein vineyard is located on the Elbe valley and has a rather steep slope consisting of three main terraces with several mini-terraces. We needed to implement the DEM for the vineyard in order to take the slope into account. We uploaded a 20 cm resolution orthophoto, and a 1 m resolution DEM for the model vineyard (data available on Geoportal Sachsen 2016a,b). As ENVI-met has a minimum vertical resolution of 1 m for the DEM, it is not able to model continuous slopes. Thus, we simplified the raw DEM to obtain three main terraces with several mini-terraces and with one grapevine row per mini-terrace (Fig. 6).

Table 5: Granite parameters used for the implementation of wall parameters in ENVI-met.

Tabelle 5: Verwendete Parameter für den Granit zur Implementierung der Mauerparameter in ENVI-met.

Property	Value used	Reference
Reflection	0.30	(Dobos 2011)
Absorption	0.70	(Dobos 2011)
Emissivity	0.45	(Engineering ToolBox 2003b)
Specific Heat	790 J/(kg*K)	(Engineering ToolBox 2003c)
Thermal conductivity	3.07 W/(m*K)	(Cho et al. 2009)
Density	2750 kg/m ³	(Engineering ToolBox 2003a)

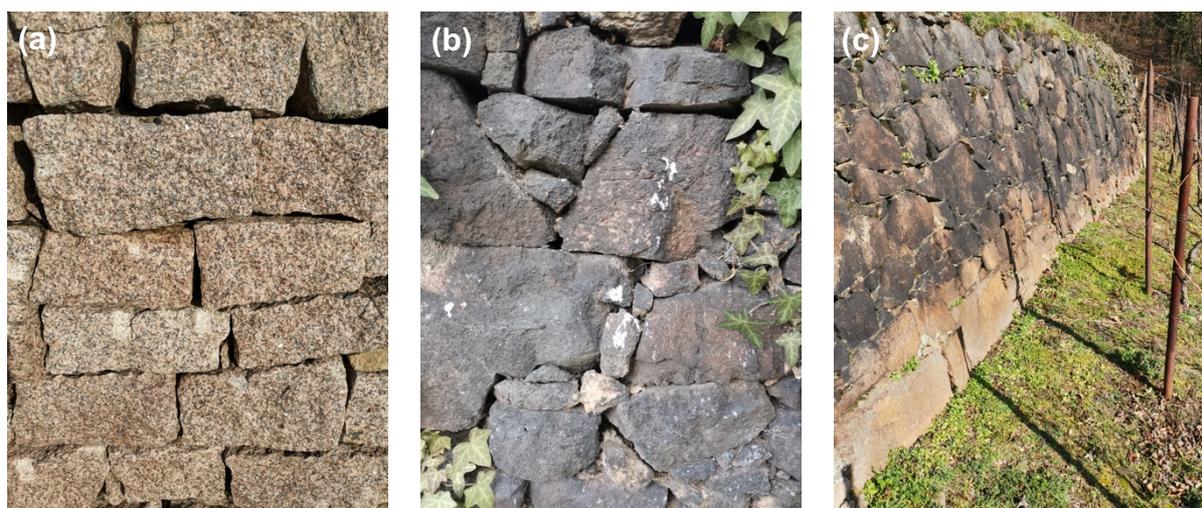


Fig. 5: Pictures showing vineyard walls of different age and color: (a) new wall, (b) old wall, (c) wall with different alteration degree (Photos: A. Noirault).

Abb. 5: Fotos von Weinbergsmauern unterschiedlicher Alterung und Färbung: (a) neue Mauer, (b) alte Mauer, (c) Mauer mit verschiedenen Verfärbungen (Fotos: A. Noirault).

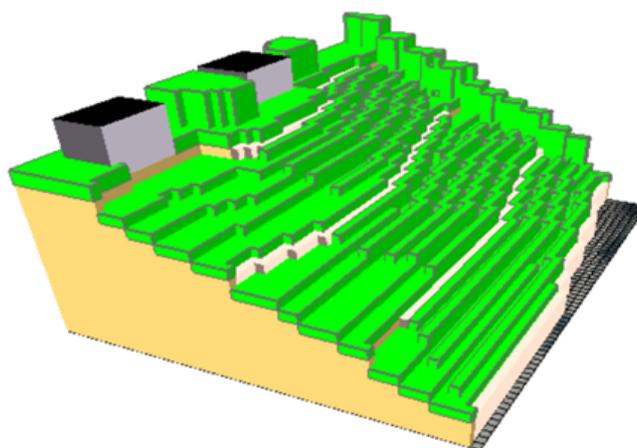


Fig. 6: Model of the chosen study vineyard. This is a DEM of 1 m resolution with three terraces and several mini-terraces with one grapevine row each.

Abb. 6: Modell des ausgewählten Testweinbergs. Es zeigt ein Höhenmodell von 1m Auflösung mit drei Hauptterrassen des Weinbergs und mehreren Kleinterrassen mit jeweils einer Rebzeile.

3.5 Creation of the 3D-model with SPACES

The first step for modelling was to create an .INX file by the Spaces ENVI-met module. We created a grid with the same dimensions as the modelled part of the Friedstein vineyard, i.e., $x = 65$ m, $y = 49$ m. We then chose $z = 39$ and a horizontal resolution $dz = 1$ m with a telescoping factor of 20 % above a height of 16 m. These values enable a model top at 314.63 m and ensure a higher resolution in the first/lower layers where grapevines are present.

To design the 3D models and enable comparisons between different scenarios of interest, we used a simplified basic model of a vineyard. We started by creating this basic model with the DEM, the grapevine rows, walls, and buildings at the same positions as in reality (see Fig. 1). To place grapevine rows and walls we used a 20 cm orthophoto (Geoportal Sachsen 2016b) imported into SPACES. We finally added a soil profile corresponding to the vineyard soil of the model vineyard (see above). The definition of the scenarios to test the different conditions was made by modifying this basic file (addition of particular ground cover, modification of wall colour). Fig. 6 shows the .INX file corresponding to a complete ground cover.

4. Results I: Sensitivity analysis

4.1 Objectives and Principles

The parameters which have to be defined in the ENVI-met database before starting the simulation are shown in Table 6. Among these input parameters some are kept constant in the different scenarios and model configurations. Then, in order to understand how the parameters affect the results, i.e. to what extent ENVI-met is sensitive to these parameters, we conducted a sensitivity analysis with variation of parameters.

Table 6: Parameters defined in the ENVI-met database manager.

Tabelle 6: Verwendete Parameter im ENVI-met Datenbankmanager.

Climatical variables	Vegetation parameters	Soil and wall physical properties
Constant parameters		
Relative air humidity	LAD LG	Soil profile
Wind speed at 10 m	LAD HG	Soil roughness
Wind direction	LAD grapevine	Soil emissivity
Soil moisture 0-20 cm	LAD LG + grapevine	Wall thickness
Soil temperature 0-20 cm	LAD HG + grapevine	Wall height
Variable parameters		
Initial air temperature	Ground cover height	Wall albedo
	Ground cover albedo	Soil albedo
	Ground cover LAD	

4.2 Procedure of the sensitivity analysis

In the sensitivity analysis we focussed on the variable parameters defined in Table 6. In a first step we defined the variation range of each parameter (Table 7). For soil, granite and ground cover albedo we got data from the literature (Dobos 2011). For the range of initial air temperature we used the maximum and minimum daily mean air temperature obtained from the German climate data centre (DWD 2020). For the LAD we used our own calculated data (see 3.1) for several vegetation types to estimate a range. The values used in the sensitivity analysis were chosen in order to have a high and a low value and to have a simple relation between these values (e.g. x5, x10, +50 %) (Table 7). Finally, we computed two different simulation scenarios (using the two extreme values defined in Table 7) for each of the seven parameters tested. All the other parameters were kept constant so that the variation in micro-climatic parameters between the two scenarios can only be explained by the parameter in variation. The initial values implemented for all 14 scenarios are shown in Table 8.

For the sensitivity analysis, we chose a simplified 3D-area to reduce the run-time for the simulations and to make the interpretation of the results easier. We designed a flat vineyard with three grapevine rows and a single wall (Fig. 7). The dimensions of the grid used are $x = 15$ m, $y = 10$ m and $z = 30$ m. The horizontal resolution is $dz = 0.5$ m.

Table 7: Common observed range and minimum/maximum values used for each parameter tested during the sensitivity analysis.

Tabelle 7: Allgemein bekannter Wertebereich und verwendete Minimal-/Maximalwerte in der Sensitivitätsanalyse.

Parameter	Common range	Chosen low value	Chosen high value
Initial air temperature	-2°C to 28°C	12.4	22.4
Ground cover height	5 – 100 cm	10	100
Ground cover albedo	0.16 – 0.27	0.18	0.27
Ground cover LAD	0.5 – 4.0 m ² /m ³	0.5	5.0
Wall albedo (granite)	0.15 – 0.35	0.15	0.30
Soil albedo	0.05 – 0.50	0.05	0.50
Ground cover	0 – 100 %	0	100

Table 8: Summary of tested parameters and initial conditions used in each simulation scenario of the sensitivity analysis. **Bold** = low and high values of each parameter tested (see Table 7).

Tabelle 8: Überblick über getestete Parameter und verwendete Anfangsbedingungen für jedes Simulationsszenario der Sensitivitätsanalyse. **Fett** = niedriger und hoher Wert des jeweils getesteten Parameters (Table 7).

Parameter	Initial air temp. (°C)	Ground cover height (cm)	Ground cover albedo	Ground cover LAD (m ² /m ³)	Wall albedo (granite)	Soil albedo	Ground cover (%)
Low initial air temperature	12.4	20	0.2	1	0.3	0.16	100
High initial air temperature	22.4	20	0.2	1	0.3	0.16	100
Low ground cover height	20	10	0.2	1	0.3	0.16	100
High ground cover height	20	100	0.2	1	0.3	0.16	100
Low ground cover albedo	20	20	0.18	1	0.3	0.16	100
High ground cover albedo	20	20	0.27	1	0.3	0.16	100
Low ground cover LAD	20	20	0.2	0.5	0.3	0.16	100
High ground cover LAD	20	20	0.2	5	0.3	0.16	100
Low wall albedo (granite)	20	20	0.2	1	0.3	0.16	100
High wall albedo (granite)	20	20	0.2	1	0.15	0.16	100
Low soil albedo	20	20	0.2	1	0.3	0.05	100
High soil albedo	20	20	0.2	1	0.3	0.5	100
Ground cover	20	20	0.2	1	0.3	0.16	100
Ground cover	20	20	0.2	1	0.3	0.16	0

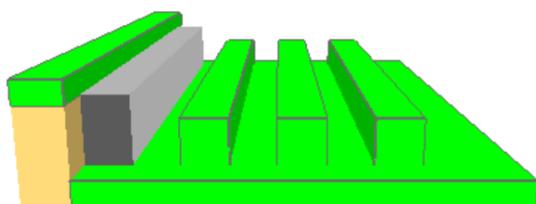


Fig. 7: Picture of the vineyard model used in the sensitivity analysis (one terrace, one wall, three rows of grapevines).

Abb. 7: Darstellung des in der Sensitivitätsanalyse verwendeten Weinbergmodells (eine Terrasse, eine Mauer, drei Rebzeilen).

We run all these models in ENVI-met for a single day and we analysed the results with Leonardo. To analyse the results and understand the sensitivity of ENVI-met to each parameter we compared the two models of a pair (comparison of the outputs obtained between a model with a low value for the tested input parameter and another model with a high value for this parameter). Leonardo enables the comparison of two models by calculating the relative change between the two resulting microclimate variables.

The first step for each model was to determine at which time of the day the difference between the two models was the highest. For most of the tested parameters, the highest difference in micro-climate was observed around 1.00 p.m. or 2.00 p.m. Thus, we used the results from these times of day to analyse the sensitivity of our model to the various parameters. The second step was to calculate the relative change for several climatic variables between the two models of each pair. Indeed, the sensitivity of ENVI-met to a parameter may be different for each climate variable. For instance, solar radiation, air temperature or leaf temperature could be differentially affected by the input parameters and consequently sensitivity would be different for the various climate variables. We decided to analyse the relative change for several micro-climatic and physiological variables: air temperature, relative humidity, solar reflection, leaf temperature, vapor flux, CO₂ flux and stomatal conductance. Finally, we studied the relative change between models of the seven variables at three different heights from ground level to 1 meter, because the highest differences were always observed in these base layers. We only considered the maximum relative change for each micro-climatic or physiological variable among all vertical layers studied.

After extracting the relative change, the sensitivity was calculated by dividing the percentage change in output by the percentage change in input. We calculated the sensitivity of each micro-climatic or physiological variable for each parameter tested. The analysis of the results was done in two different ways: For each parameter we analysed which microclimatic or physiological variable was the most affected; for each microclimatic or physiological variable we analysed which parameter was the most influential.

4.3 Results of the sensitivity analysis

Table 9 shows that the sensitivity of each output variable highly depends on the input parameter. For example, air temperature is highly affected by the initial temperature of the model (sensitivity = 0.48) but, it is nearly insensitive to the other parameters (sensitivity < 0.1). On the contrary, the sensitivity to a given parameter highly depends on the output variable in study. For instance, wall albedo highly affected solar reflection, but had almost no effect on leaf or air temperature. The most sensitive variables were stomatal resistance, solar reflection and CO₂ flux, whereas relative humidity, vapor flux and leaf temperature are the least sensitive variables in regard to the input parameters used (Table 9). As a result of the sensitivity analysis, soil albedo showed no effect on any of the output variables, ENVI-met may not take it into account when vegetation is present. Finally, as the totality of sensitivity values were smaller than 1, in all cases the percentage variation in output variables is reduced compared to the percentage variation in initial parameters.

Table 9: Sensitivity of each output variable to the seven tested input parameters. **Bold** = highest sensitivity for each tested parameter.

Tabelle 9: Sensitivität der simulierten Variablen gegenüber den sieben getesteten Eingangsparametern. **Fett** = höchste Sensitivität des jeweils getesteten Parameters.

Parameter	Variable						
	Air temp.	Relative humidity	Solar reflection	Leaf temp.	Vapor flux	CO ₂ flux	Stomatal resistance
Vegetation albedo	0.05	0.16	0.00	0.04	0.08	0.16	0.25
Vegetation height	0.01	0.02	0.12	0.00	0.00	0.01	0.02
Vegetation LAD	0.01	0.6	0.22	0.02	0.02	0.04	0.11
Wall albedo	0.01	0.02	0.27	0.02	0.03	0.07	0.09
Soil albedo	0.00	0.00	0.00	0.00	0.00	0.00	0.00
Initial temperature	0.48	0.26	0.02	0.31	0.09	0.53	0.48
Ground cover	0.02	0.11	0.41	0.06	0.20	0.34	0.56

If one studies which output variable is the most affected for each input parameter, it can be shown that vegetation albedo mostly affects stomatal resistance (sensitivity = 0.25) whereas vegetation height and LAD mainly affect solar reflection. Wall albedo mainly affects solar reflection and initial temperature, which is the most influential input parameter, affecting grapevine's physiological variables CO₂ flux, stomatal resistance and leaf temperature as well as air temperature and relative humidity (Table 9). Furthermore, it could be shown that the presence of ground vegetation mostly affects stomatal resistance but also solar reflection.

We transformed the absolute values from the previous table to get values in percentages of the total sensitivity (Table 10). In this way we could assess the portion of output variation explained by a given parameter. This enables to understand which parameter is the most influential for each output variable. As expected, for air temperature the most influential input parameter was the initial value chosen for temperature, representing more than 80 % of the variation explained by the tested input parameters (Table 10). This was also true for relative humidity (40 % of the variation explained, Table 10) due to the interrelationship between relative humidity and air temperature. These conclusions must also apply to vapor pressure deficit (VPD) as it considers both parameters. Vegetation characteristics explained around 13 % of the variation in air temperature and particularly vegetation albedo explained almost 40 % of the variation in relative humidity (Table 10). Solar reflection is highly affected by wall albedo and the presence or absence of vegetation. This was expected as these two parameters correspond to variation in solar reflectivity properties (granite and "soil" albedo). However, vegetation albedo has almost no effect on reflected radiation (Table 10) which indicates that vegetation LAD is more important as it represents structural complexity and can explain a great part of the absorption. Concerning the vine physiological parameters calculated by ENVI-met, vine leaf temperature is mainly influenced by initial air temperature, but also to a much lesser extent by presence of vegetation cover. Vapor flux, CO₂ flux and stomatal resistance are quite similar and highly sensitive to presence of vegetation cover and initial air temperature (Table 10).

Table 11 shows that vegetation characteristics affect climate parameters in the same way. Relative humidity was proportional to vegetation height, LAD and albedo, whereas air temperature, leaf temperature and stomatal resistance were inversely proportional to these parameters. Solar reflection and leaf temperature both increased with wall albedo, the presence of vegetation increased relative humidity, but decreased solar reflection. We can also see dependencies between variables: For instance, when air temperature decreases, leaf temperature decreases too and relative humidity increases; when stomatal resistance is lower, vapor flux and plant CO₂ flux increase.

Table 10: Percentages of explained variation related to total variation explained by the tested parameters. The sum of the percentage of each column is 100 %. **Bold** = Percentage of to the most influential parameter for each output variable.

Tabelle 10: Prozentanteile der erklärten Varianz bezogen auf die erklärte Gesamtvarianz pro getestetem Parameter. Die Summe jeder Spalte ergibt 100 %. **Fett** = Prozentanteil des Parameters mit dem höchsten Einfluss auf die jeweilige Variable.

Parameter	Variable						
	Air temp.	Relative humidity	Solar reflection	Leaf temp.	Vapor flux	CO ₂ flux	Stomatal resistance
Vegetation albedo	9.01	25.62	0.12	9.05	18.24	13.97	16.69
Vegetation height	2.16	3.74	11.37	0.91	0.57	0.95	1.39
Vegetation LAD	2.03	9.50	21.48	3.63	4.47	3.84	7.25
Wall albedo	1.25	3.36	25.65	3.79	7.94	6.35	6.19
Soil albedo	0.00	0.00	0.00	0.00	0.00	0.00	0.00
Initial temperature	82.18	40.96	1.58	69.45	20.67	45.45	31.54
Ground cover	3.36	16.82	39.81	13.17	48.10	29.43	36.95

Table 11: Summarized overview of the relationships between input parameters and output variables. ↗ positive relationship, ↘ negative relationship, – no effect.

Table 11: Zusammenfassende Übersicht über die Beziehungen zwischen Eingangsparametern und den Output-Variablen. ↗ positive Beziehung, ↘ negative Beziehung, – kein Effekt.

Parameter	Variable					
	Air temperature	Relative humidity	Solar reflection	Leaf temperature	Vapor flux	CO ₂ flux
Vegetation albedo	↘	↗	–	↘	↗	↗
Vegetation height	↘	↗	↘	↘	↗	↗
Vegetation LAD	↘	↗	↘	↘	↗	↗
Wall albedo	↗	↘	↗	↗	↘	↘
Initial temperature	↗	↘	↗	↗	↗	↘
Presence of vegetation	↘	↗	↘	↘	↗	↗

5. Results II: Modelling results for the micro-climate

5.1 Temporal variation of microclimatic and physiological parameters

5.1.1 Daily courses at a point in the vineyard

Fig. 8 shows the daily courses of several climatic variables for a single grid point in the centre of the model vineyard and for the chosen summer day (here 18th, July, 2019).

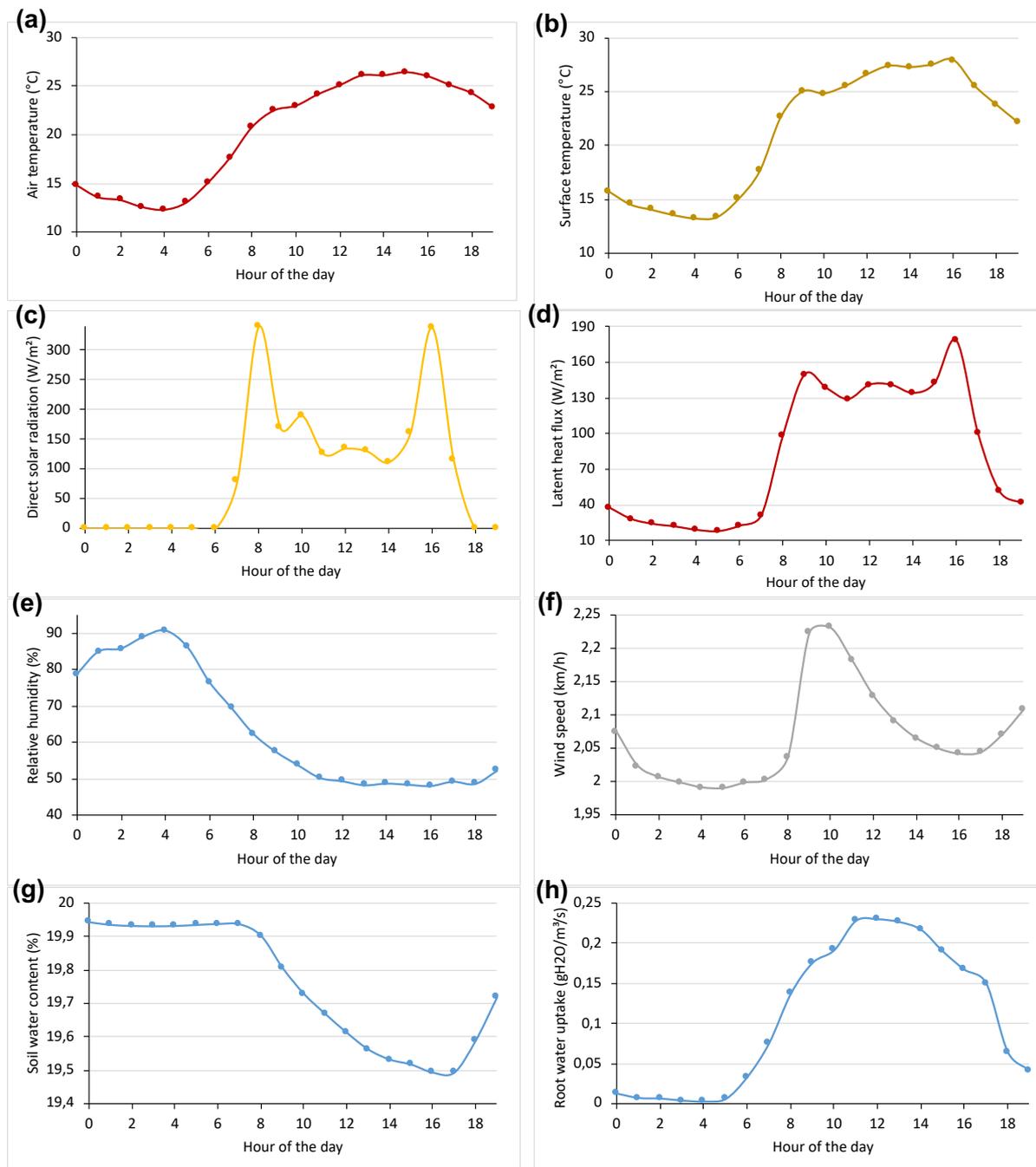


Fig. 8: Daily courses of microclimatic variables, energy and water fluxes modelled for one pixel (1 m x 1 m) in the center of the vineyard (middle terrace, interrow): (a) air temperature, (b) surface temperature, (c) direct solar radiation, (d) latent heat flux, (e) relative humidity, (f) wind speed, (g) soil water content, (h) root water uptake.

Abb. 8: Tagesläufe der mikroklimatischen Variablen modelliert für ein Pixel (1 m x 1 m) im Zentrum des Weinbergs (mittlere Terrasse, Rebgasse): (a) Lufttemperatur, (b) Oberflächentemperatur, (c) direkte Sonneneinstrahlung, (d) latenter Wärmefluss, (e) relative Luftfeuchtigkeit, (f) Windgeschwindigkeit, (g) Bodenwassergehalt, (h) Wasseraufnahme der Wurzel.

As can be seen in Fig. 8, air temperature increases from 6:00 am to 3:00 pm when surface temperature increases until 4:00 pm (Fig. 8a and 8b). Direct solar radiation is only present during the day from 6:00 am to 6:00 pm (Fig. 8c). At the same time, latent heat flux is found to be the highest during the day and is almost null during the night (Fig. 8d). On the contrary, soil water content and relative humidity are the highest during the night and decrease during the day respectively from 5:00 am and 8:00 am to 4:00 pm (Fig. 8e and 8g). Wind speed is almost constant around 2 km/h during the whole daily course (Fig. 8f). Finally, root water uptake increases from 6:00 am to midday and then decreases until the night (Fig. 8h).

Fig. 9 shows the daily course for several physiological parameters of the vine plants. Leaf temperature increases from 5:00 am to 3:00 pm before decreasing until the night (Fig. 9a). Stomatal conductance increases rapidly at 6:00 am and then stays high until 6:00 pm when it decreases to reach its initial low level (Fig. 9b). CO₂ flux, which is a proxy for grapevine photosynthesis, increases from 8:00 am to midday before decreasing slowly until the end of the day (Fig. 9c). Vapor flux also increases from 8:00 am to 1:00 pm before decreasing in the afternoon (Fig. 9d). On the contrary, water use efficiency follows an inverse pattern as it shows a minimum at 1:00 pm (Fig. 9f). Finally, vapor pressure deficit increases from 4:00 am to 3:00 pm before decreasing until the night.

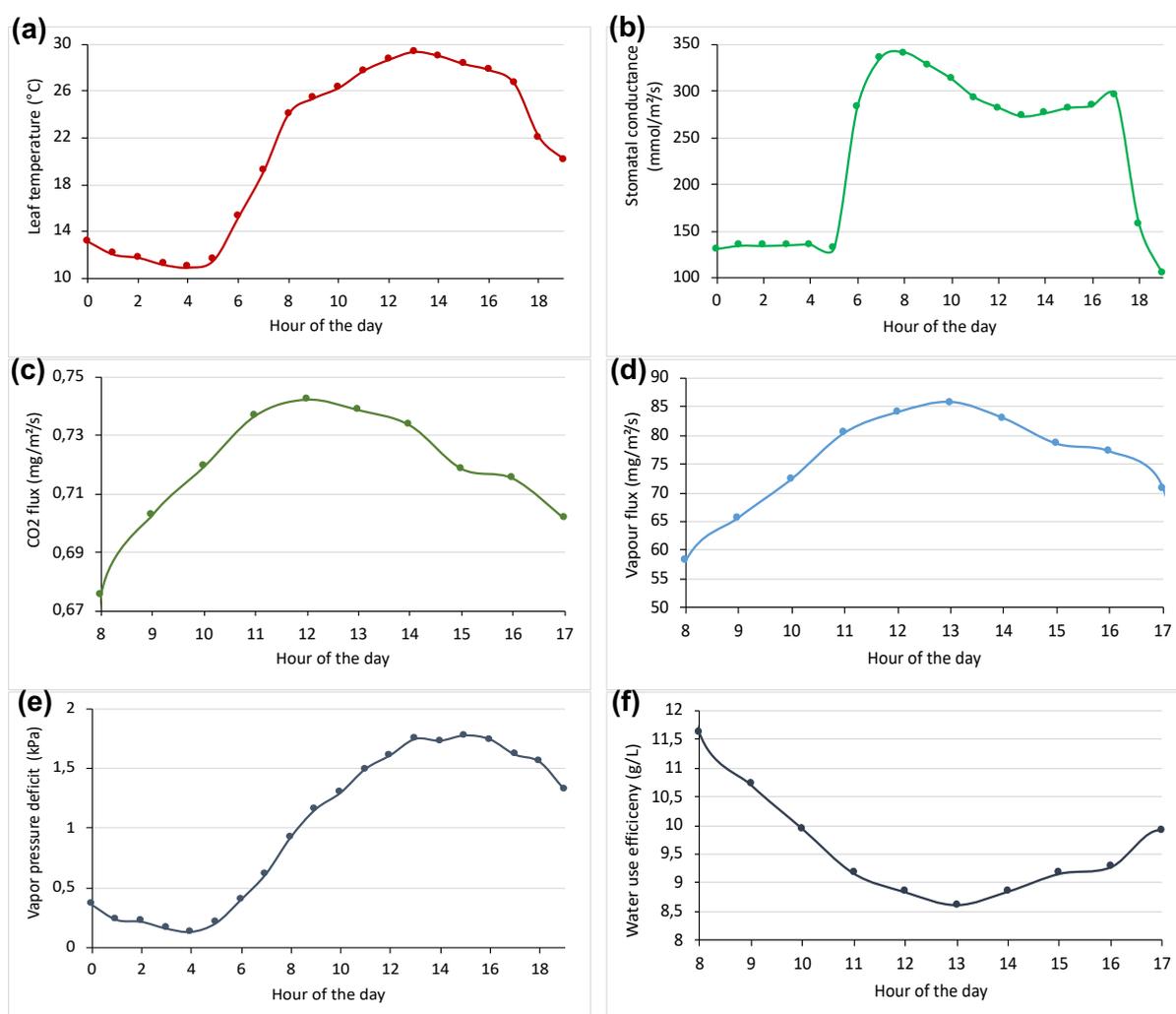


Fig. 9: Daily courses of atmospheric and plant physiological quantities modelled for one pixel (1 m x 1 m) in the center of the vineyard (second terrace, interrow): (a) leaf temperature, (b) stomatal resistance, (c) CO₂ flux, (d) vapor flux, (e) vapor pressure deficit, (f) water use efficiency.

Abb. 9: Tagesläufe atmosphärischer und physiologischer Größen modelliert für ein Pixel (1 m x 1 m) im Zentrum des Weinbergs (mittlere Terrasse, Rebgasse): (a) Blatttemperatur, (b) stomatärer Widerstand, (c) CO₂-Fluss, (d) Wasserdampfdruck, (e) Wasserdampfättigungsdefizit, (f) Wassernutzungseffizienz.

5.1.2 Daily courses of selected parameters on average in the vineyard

Vineyard microclimate under a typical current July day was simulated with ENVI-met for one day (here 18th, July, 2019). Fig. 10 shows the results obtained for several micro-climatic variables and some grapevine physiological parameters as average from all pixels in the vineyard. Average air temperature and leaf temperature showed a similar daily course (Fig. 10a) and were also positively correlated. The minimum temperature value (< 15°C) was found during the early morning at 4:00 am and the maximum value (> 25°C) in the afternoon at 2:00 am to 3:00 am (Fig. 10a). On the contrary, relative humidity was highest during the early morning and decreased during the day (Fig. 10a). Not surprisingly, stomatal conductance of grapevine leaves and CO₂ flux both were higher during the day than during the night (Fig. 10b). The increase in stomatal conductance and hence photosynthesis indicated by CO₂ flux started with sunrise between 6:00 and 7:00 am, reached a plateau between 8:00 am and 5:00 pm and then decreased again until 7:00 pm (Fig. 10b). As transpiration is also correlated with stomatal conductance, vapor flux and vapor pressure deficit (VPD) showed similar daily courses (Fig. 10c): Both variables increased from 6:00 am to 3:00 pm and then decreased again.

5.2 Spatial variation of microclimatic and physiological parameters

Fig. 11 shows the spatial variation of micro-climatic variables and physiological parameters in the model vineyard on a specific time of the chosen summer day as LEONARDO output. Air temperature (Fig. 11a) was quite homogenous in the vineyard between 25°C and 26°C. However, within the core of the vineyard with a south-eastern aspect, air temperature was up to 1°C higher than at the borders of the vineyard (Fig. 11a). Surface temperature obviously depends on the presence of grapevine as it was up to + 4°C higher under the vine plants (Fig. 11b). Direct solar radiation showed a similar spatial pattern with lower values below grapevines and the highest between vine rows (Fig. 11c). Specific humidity (Fig. 11d) as well as soil wetness (Fig. 11e) were higher in the upper terraces (+20 % in comparison to the lowest terrace). Moreover, soil wetness was slightly reduced under grapevines. Wind speed was lower in the planted parts (core) of the vineyard compared with the unplanted area at the borders (Fig. 11f).

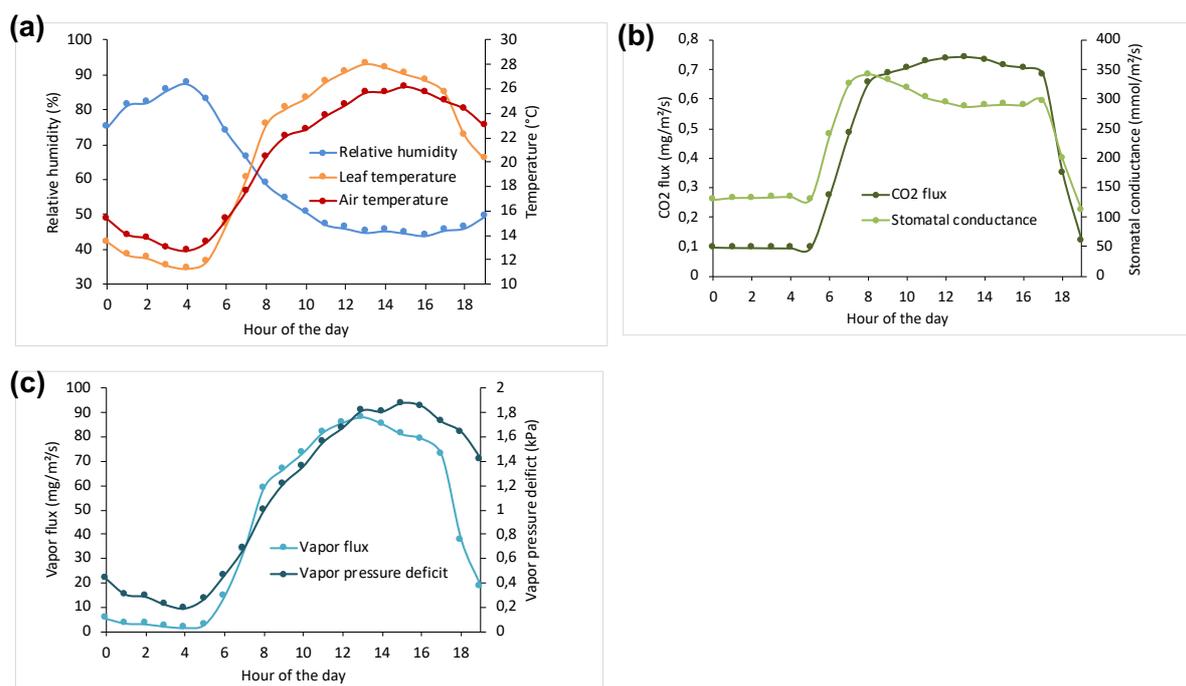


Fig. 10: Daily courses of micro-climatic and physiological parameters in the model vineyard obtained with ENVI-met (average values for the whole area): (a) air temperature (°C), relative humidity (%) and vine leaf temperature (°C); (b) transpiration (vapor flux) (mg/m²/s) and vapor pressure deficit (VPD) (kPa), (c) CO₂ assimilation flux (mg/m²/s) and stomatal conductance (mmol/m²/s). Vineyard completely covered with low-growing vegetation under a current typical day of July (here: 18th July, 2019).

Abb. 10: Tagesläufe der mikroklimatischen und physiologischen Parameter (Wein) im Modellweinberg berechnet mit ENVI-met (Mittelwerte über die gesamte Fläche): (a) Lufttemperatur (°C), relative Luftfeuchtigkeit (%) und Blatttemperatur (Wein); (b) Transpiration (Wasserdampftransport) (mg/m²/s) und Wasserdampfdruckdefizit (kPa), (c) CO₂-Fluss (mg/m²/s) und stomatare Leitfähigkeit (mmol/m²/s). Weinberg komplett mit niedrigwüchsiger Vegetation bewachsen, typischer Julitag (hier: 18. Juli 2019).

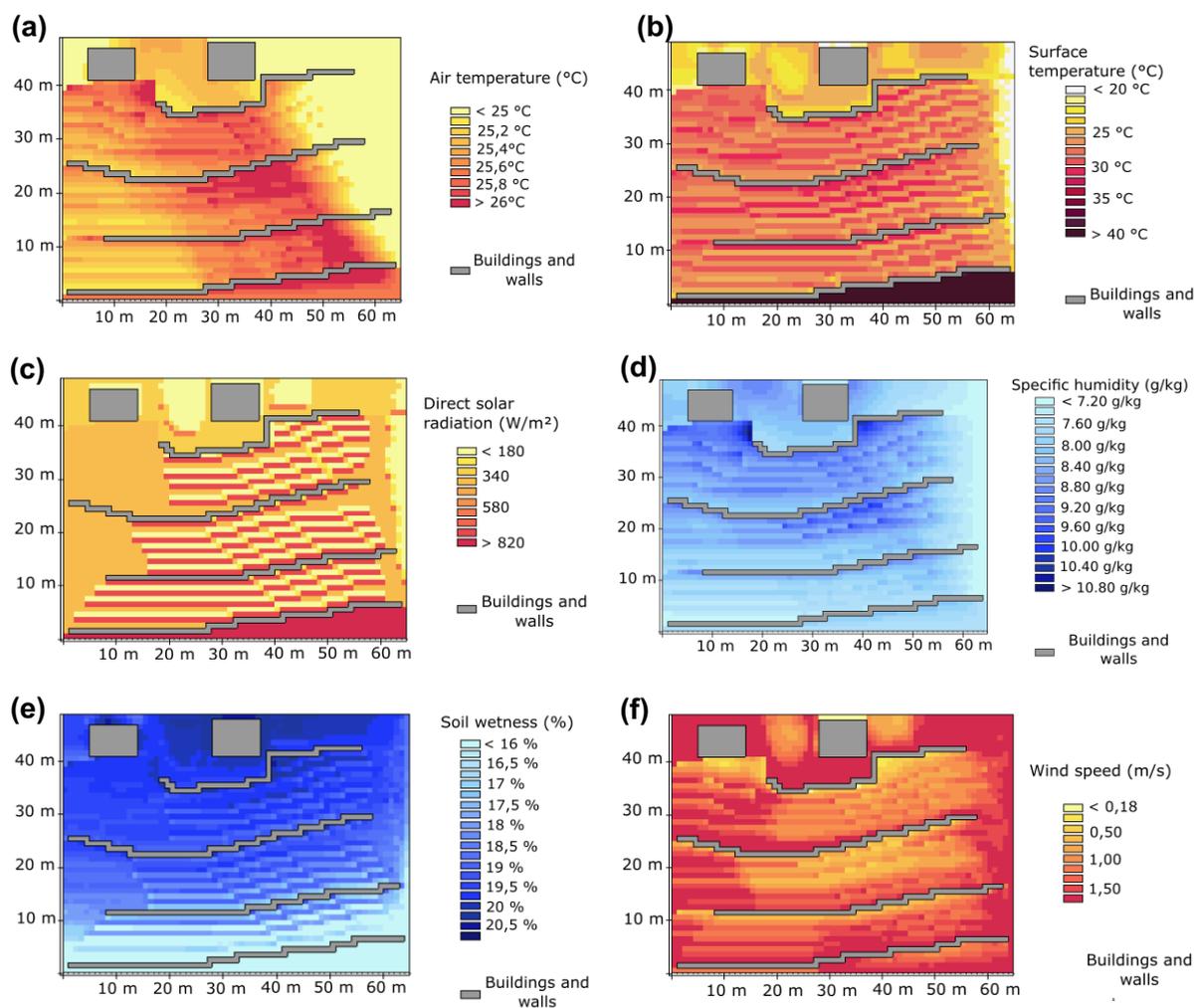


Fig. 11: Spatial distribution of microclimatic and soil characteristics simulated with ENVI-met: (a) air temperature at 1:00 pm, (b) surface temperature at 1:00 pm, (c) direct solar radiation at 1:00 pm, (d) specific humidity at 1:00 pm, (e) soil wetness at 5:00 pm, (f) wind speed at 1:00 pm. Vineyard completely covered with low-growing vegetation under a current typical day of July (here: 18th July, 2019). Grey = vineyard walls and buildings.

Abb. 11: Räumliche Verteilung von mikroklimatischen und Bodeneigenschaften simuliert mit ENVI-met: (a) Lufttemperatur um 13:00 Uhr, (b) Oberflächentemperatur um 13:00 Uhr, (c) Direkte Sonneneinstrahlung um 13:00 Uhr, (d) spezifische Luftfeuchte um 13:00 Uhr, (e) Bodenfeuchte um 17:00 Uhr, (f) Windgeschwindigkeit um 13:00 Uhr. Weinberg komplett mit niedrigwüchsiger Vegetation bewachsen, typischer Julitag (hier: 18. Juli 2019). Grau = Weinbergsmauern und Gebäude.

Fig. 12 shows the LEONARDO results of the calculated grapevine parameters. Corresponding to air temperature (Fig. 11a), vine leaf temperature (Fig. 12a) was slightly higher on the middle and upper main terrace and in the parts with south-eastern aspects; the lowest terrace showed the lowest leaf temperature. Simultaneously, stomatal conductance (Fig. 12b) was higher in the highest terrace. As a result, CO₂ assimilation (CO₂ flux, Fig. 12c) was increased in the highest terrace, but to a very small amount. Interestingly, transpiration shown as vapor flux (Fig. 12d) seems to increase with the distance from the wall which might be an effect of the higher ventilation (higher wind speed) and the lower air humidity (specific humidity) away from the wall (Fig. 12d et Fig. 13). In addition, vapor flux was also slightly higher in the lower terrace compared with the middle and the upper terrace (Fig. 12d). As already shown in Fig. 11f, wind speed seems to be reduced in the (planted) core of the vineyard (Fig. 13), particularly near the walls. Moreover, wind direction was influenced by the walls and vine rows as its direction becomes nearly parallel to the walls and the rows within the core of the vineyard.

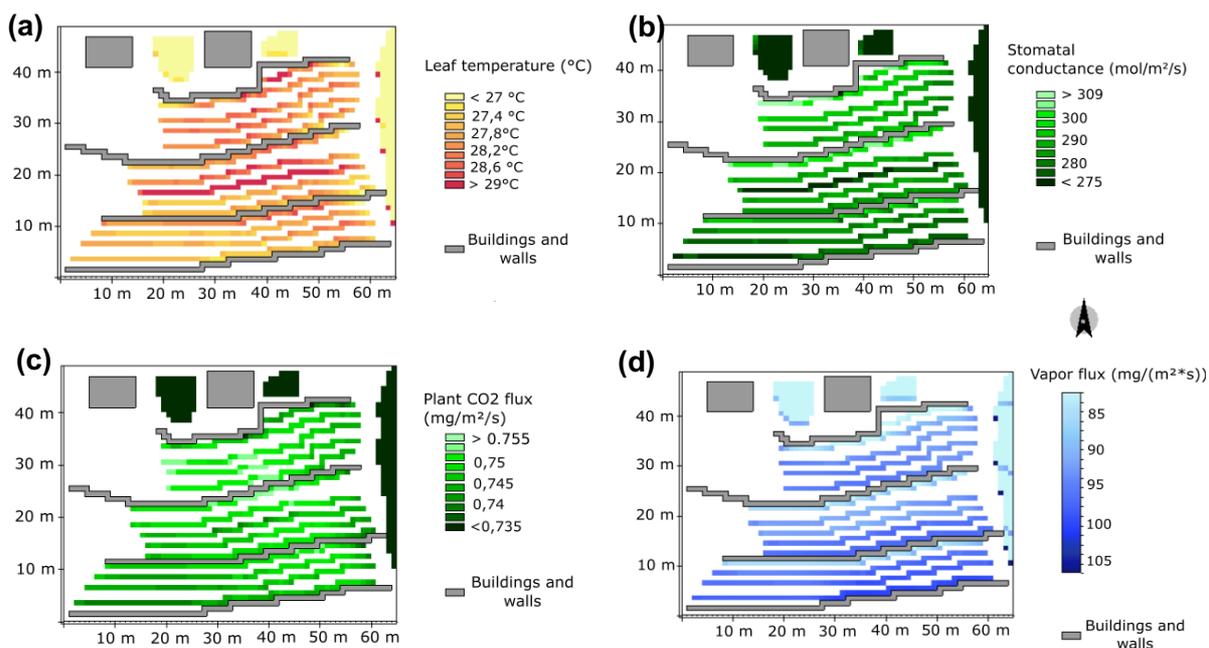


Fig. 12: Spatial distribution of grapevine physiological parameters simulated with ENVI-met. The simulation was made with a vineyard completely covered with low-growing vegetation under a typical day of July (here: 18th, July, 2019; see methods): (a) air temperature at 1:00 pm, (b) stomatal conductance at 1:00pm, (c) plant CO₂ flux at 1:00pm, (d) vapor flux at 1:00pm. Vineyard completely covered with low-growing vegetation under a current typical day of July (here: 18th July, 2019). Grey = vineyard walls and buildings; parallel lines: vine rows.

Abb. 12: Räumliche Verteilung der physiologischen Parameter (Wein) simuliert mit ENVI-met: (a) Lufttemperatur um 13:00 Uhr, (b) stomatärer Leitfähigkeit um 13:00 Uhr, (c) CO₂-Fluss (Netto-Photosynthese) um 13:00 Uhr, (d) Wasserdampffluss (Transpiration) um 13:00 Uhr. Weinberg komplett mit niedrigwüchsiger Vegetation bewachsen, typischer Julitag (hier: 18. Juli 2019). Grau = Weinbergsmauern und Gebäude, parallele Linien: Rebzeilen.

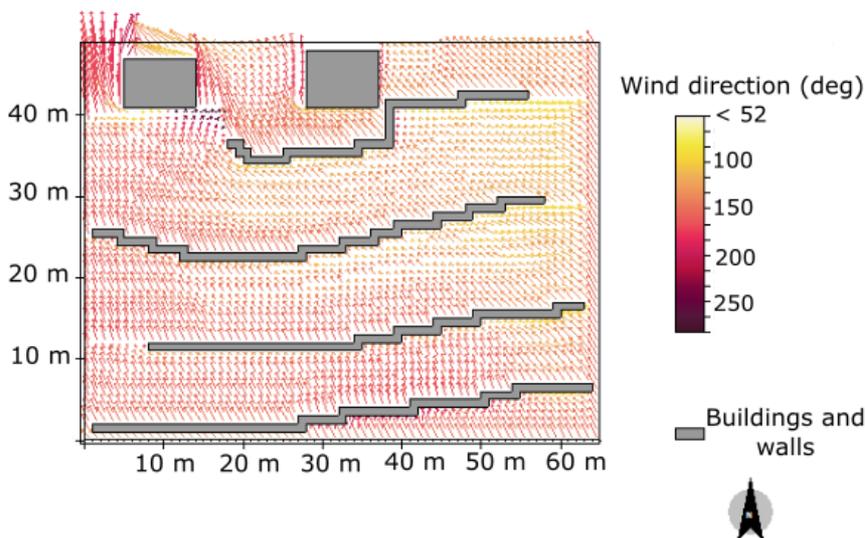


Fig. 13: Wind directions (direction of the arrows) and wind speed (proportional to the length of the arrows) simulated with ENVI-met for the vineyard covered with low-growing vegetation under a current typical day of July (here: 18th July, 2019).

Abb. 13: Windrichtungen und Windgeschwindigkeiten (Länge der Pfeile) simuliert mit ENVI-met für den Weinberg mit niedrigwüchsiger Vegetation bewachsen, typischer Julitag (hier: 18. Juli 2019).

5. Discussion

To our knowledge, the ENVI-met software had been mostly used for urban areas up to now. Among other topics, it has been used to investigate potential solutions to avoid or reduce urban heat islands (Ambrosini et al. 2014; Deilami et al. 2018). Some other studies also focused on the effect of climate change on urban microclimate (Huttner et al. 2008). In this study, we tested whether this computer program, initially designed for urban areas, can also be used for simulating microclimate in vineyards. For this purpose, we first created a three-dimensional model of an existing vineyard (Friedstein, Radebeul). Using the ENVI-met database and the SPACES software,

we obtained a simplified structure, but consistent with reality (Fig. 6). Second, the plot structure and initial settings were suitable to stabilize the model (chapter 3) and to run simulations.

In order to use ENVI-met for applications in vineyards, understanding the sensitivity of the model to the input data is very important. For this purpose, we calculated the sensitivity of the calculated output variables to the input parameters used in a sensitivity analysis (chapter 4). Among other results, we found that the chosen initial temperature is the most impacting input parameter for each climate variable estimated as it greatly influences air temperature, leaf temperature but also many physiological processes such as transpiration and photosynthesis (Table 10). This was also found in the literature and it has been proven that both transpiration and photosynthesis of vines are positively correlated with air temperature within the observed temperature range (see Greer 2012).

The presence of a ground vegetation cover is also a factor of influence, in particular for the vineyard's water status (soil water content, relative humidity, stomatal resistance, vapor flux, Table 10, 11). This might be due to the root system of the ground cover species and to the effect of the vegetation cover on solar radiation. Among the vegetation characteristics it appears that vegetation albedo is the most influential input parameter on microclimate outputs in comparison with vegetation LAD and vegetation height (Table 9). However, vegetation height and LAD seem to be more important for solar reflection than vegetation albedo (Table 9). A possible explanation could be that a higher LAD or height of the ground cover vegetation may be responsible for a higher absorption, which would reduce solar reflection (see Bruse 2004) for model equations and reduction coefficients considering absorption). Solar reflection also decreases when vegetation is present (Table 11). This is also surprising as vegetation albedo is higher than soil albedo, but, on the other hand, absorption may be more important as ground structure is more complex with vegetation. In fact, a large part of solar radiation is absorbed or transmitted through vegetation following Beer's law. This is well described in the manual of ENVI-met (Bruse 2004). Then, as expected, wall albedo was highly important for solar reflection (Table 10) which may result in a great influence on several microclimatic and physiological variables, at least next to the walls. Finally, it is worth noting that, soil albedo is not important when there is vegetation maybe because most of solar radiation is already absorbed by vegetation before reaching the soil for partial reflection.

In conclusion, we can deduce from the results of our sensitivity analysis that the most sensitive variables were stomatal conductance, solar reflection, and CO₂ flux whereas relative humidity, vapor flux and leaf temperature were the least sensitive variables. It should be noted that the obtained sensitivity values all were inferior to 1 what means that in all cases the percentage variation in resulting climate is lower than the percentage variation in initial parameters. There is a wide range of climate and physiological variables which can be obtained as outputs of the simulations in ENVI-met. Among them, some are common such as air temperature and relative humidity, others are more specific such as stomatal conductance or water use efficiency. The results obtained for the daily courses of the studied climate variables (chapter 5.1) were consistent with the expectations and no unrealistic values were found for any of the variables and scenarios. Although we could not compare these results with field measurements yet (see below), the obtained values seem to get along with the typical values observed in vineyards. For instance, transpiration of vines (vapor flux) is often between 20 and 100 mg/m²/s (Greer 2012) which corresponds well with our results (Fig. 9d, 10c, 12d). Values for stomatal conductance, leaf temperature or vapor pressure deficit (Fig. 9, 10, 12) were also included in the optimal range defined for plants or vines (Zeiger et al. 1987; Greer 2012; Koverda 2020). In conclusion, it appears that vineyard microclimate and grapevine condition can be confidently modelled with the ENVI-met software based on the initial parameters chosen. However, validation of the model with respect to the local structure of the vineyard would require local measurements.

For the average summer day we used in the simulations, we reproduced the already observed inverse correlation between air temperature and relative humidity (Fig. 10a; see Valsson & Bharat 2011) and the positive correlation between stomatal conductance and CO₂ flux (Fig. 10b). The latter is in accord with the results obtained by Jacobs et al. (1996) who showed that grapevine photosynthesis was correlated with stomatal conductance. Transpiration and vapor pressure deficit were also positively correlated (Fig. 10c; see Fletcher et al. 2007). Both correlations are not necessarily linear and can change with water status. Concerning the results for the spatial variation of microclimatic and physiological parameters in the model vineyard (chapter 5.2), we often found differences between the planted core of the vineyard and its unplanted margins (Fig. 11, 13). For instance, air temperature was higher within the core of the vineyard (Fig. 11a). This has also been shown by Peña Quiñones et al. (2020) who proved that the air temperature of the vineyard's canopy was higher than the air temperature measured at the closest weather station. This may be due to the radiative heat transfer between vine leaves and the surrounding air. The phenomenon of higher temperatures in the core of the vineyard could also be due to a low LAI coupled with a reduced water supply in this July day. Additionally, there might be an influence of the local topography on the spatial variation of the climate variables: Indeed, relative air and soil humidity were higher in the highest terraces (Fig. 11e, f). This could be explained by the presence of trees around the vineyard at the highest terraces, especially at the eastern border of the vineyard (Fig. 1 and 4). Due to the tree presence, wind speed may be reduced in upper terraces (Fig. 13) and this may have led to a lower and slower evaporation from the soil (see Davarzani et al. 2014). Additionally, the effect of shadowing by the high trees may also play a role. Furthermore, our results indicate that there is an influence of walls with a higher humidity observed near the walls. In addition, some physiological

parameters such as stomatal conductance (Fig. 12b) also decrease with distance to the wall. This might be due to a higher solar reflexion by the wall, especially when walls have a light colour as in our case (see wall albedo in Table 10). Finally, the grapevines planted modify microclimatic variables such as soil water content, direct solar radiation or latent heat flux. The implied shadow and the root water uptake may be responsible for the observed decrease in both soil water content (Fig. 11f) and direct solar radiation (Fig. 11c) in the planted area of the vineyard. So the ENVI-met software might be able to reveal the effect of vineyard structure and row orientation on the micro-climatic parameters and the performance of the grapevines (e.g., Griffoni et al 2008; Hunter et al 2016; 2020). All these results could be helpful to better understand spatial and daily variations in the microclimatic and physiological conditions of vineyards and grapevines, respectively.

The presented results are sufficiently reasonable to develop further applications of this computation model to vineyards. Although, field experiments and measures are needed to confirm these first results, get rid of some bias (boundary effects for instance) and the accuracy of the simulations obtained by the computer program (see Ayyad & Sharples 2019 for an example). As a potential application, one could design several scenarios with different management practices (presence/absence of ground cover, high/low ground cover, addition of trees in the vineyard, presence/absence of walls) to study the impact on the microclimate in vineyards. Even if the absolute values should be taken with care, we expect the relative changes observed between scenarios to be comparable to field observations. Furthermore, ENVI-met could also be applied to other fields. Indeed, modelling microclimate may become more and more interesting and even critical in other agricultural fields as they also may suffer from climate change in the next decades. However, of course, with this approach, one can only model the impact of some practices or structures on microclimate. In particular, the ENVI-met simulation does not allow the modelling of species interactions or long-term physiological responses that can greatly affect ecosystem functioning (Bradley & Pregitzer 2007; Brophy et al. 2017).

As a conclusion, to our knowledge we were able to model vineyard microclimate using the ENVI-met software for the first time. This has given perspectives to better understand the effect of management practices, ground vegetation and structures on vineyard microclimate and vine performance. The use of ENVI-met could offer new opportunities for winegrowers who could simulate the effect of several management strategies and adapt their management toward an optimization of vineyard microclimate and grapevine physiology particularly in a context of climate warming. It would also be necessary to support the obtained results by field measurements in future work. In any case, ENVI-met could be an appropriate research tool supporting winegrowers to implement sustainable management in their vineyards.

6. Zusammenfassung

Sachsen ist eines der nördlichsten Weinanbaugebiete in Europa. Die meisten Weinberge kommen an steilen Hängen im Elbtal vor. Daher sind die mikroklimatischen Bedingungen in den Weinbergen von enormer Wichtigkeit für den Weinbau. In dieser Arbeit wurde die Anwendbarkeit des Programms ENVI-met zur Simulation des Mikroklimas von Weinbergen getestet. Ursprünglich konzipiert für urbane Räume wurde das Programm in dieser Arbeit eingesetzt, um das Mikroklima eines typischen sächsischen Weinbergs zu simulieren. Zu diesem Zweck wurden ein 3D-Modell des Weinbergs entwickelt und die für die Simulation notwendigen Eingangsparameter zu Klima, Boden, Vegetation etc. implementiert. In diesem Beitrag werden die Ergebnisse einer Sensitivitätsanalyse und erste Ergebnisse zum Tagesverlauf und zur räumlichen Verteilung verschiedener mikroklimatischer und physiologischer Variablen präsentiert. Die anhand der Simulationen für einen typischen Sommertag (18. Juli 2019) erhaltenen Tagesläufe entsprechen den theoretischen Annahmen und Angaben aus der Literatur. Der Anwendung des Modells zur Variierung von Eingangsparametern oder Änderungen in der Weinbergsstruktur eröffnet neue Möglichkeiten, um Effekte spezieller Bewirtschaftungsmaßnahmen auf das Mikroklima und das Gedeihen der Weinreben in Weinbergen abzuschätzen.

Acknowledgements

We thank Martin Schwarz (Meißen) for providing information on the history of the Friedstein vineyard. RA, ER and BK (LandCare gGmbH) were funded by the Federal Ministry for Environment, Nature Protection, and Nuclear Safety based on a decision of Deutscher Bundestag in the framework of measures for adaptations to climate change (DAS, grant 03DAS149B, project BIODIVina: Education modules on the role of biodiversity in adaptations of viticulture to climate change).

7. Literature

- Ambrosini, D., Galli, G., Mancini, B., Nardi, I. & Sfarra, S. (2014): Evaluating mitigation effects of urban heat islands in a historical small center with the ENVI-met® climate model. *Sustainability* 6(10): 7013-7029. DOI: 10.3390/su6107013.
- American Meteorology Society (2019): Aerodynamic roughness length. AMS Glossary. URL: http://glossary.ametsoc.org/wiki/Aerodynamic_roughness_length, (accessed: 2020/03/20).

- An, N., Hemmati, S. & Cui, Y.-J. (2017): Assessment of the methods for determining net radiation at different time-scales of meteorological variables. *Journal of Rock Mechanics and Geotechnical Engineering* 9(2): 239-246. DOI: 10.1016/j.jrmge.2016.10.004
- Aragón-Durand, F., Cramer, W., Humphreys, S., Kainuma, M. & Kala, J. (2018): IPCC Special Report: Global Warming of 1.5 °C. Chapter 1. URL: <https://www.ipcc.ch/sr15/>, (accessed: 2020/07/03).
- Ayyad, Y.N. & Sharples, S. (2019): Envi-MET validation and sensitivity analysis using field measurements in a hot arid climate. IOP Conference Series: Earth Environmental Science 329: 012040. DOI: 10.1088/1755-1315/329/1/012040.
- Benyr, V. (2018, unpubl.): Analyse der Pflanzengemeinschaften sowie Kartierung der Vegetationstypen und der Blauflügeligen Ödlandschrecke auf dem neu angelegten Terrassen-Weinberg in Radebeul. Bachelorarbeit Studiengang Geoökologie, TU Bergakademie Freiberg, Institut für Biowissenschaften, 68 S. + Anhang (unpubl.).
- Bodor, P., Baranyai, L., Parrag, V. & Bisztray, G. (2014): Effect of row orientation and elevation on leaf morphology of grapevine (*Vitis vinifera* L.) c.v. Furmint. *Progress in Agricultural Engineering Sciences* 10(1): 53–69. DOI: 10.1556/Progress.10.2014.4.
- Bradley, K.L. & Pregitzer, K.S. (2007): Ecosystem assembly and terrestrial carbon balance under elevated CO₂. *Trends in Ecology & Evolution* 22(10): 538-547. DOI: 10.1016/j.tree.2007.08.005.
- Brophy, C., Dooley, Á., Kirwan, L., Finn, J.A., McDonnell, J., Bell, T., Cadotte, M.W. & Connolly, J. (2017): Biodiversity and ecosystem function: Making sense of numerous species interactions in multi-species communities. *Ecology* 98(7): 1771-1778. DOI: 10.1002/ecy.1872.
- Bruse, M. & Fleer, H. (1998): Simulating surface-plant-air interactions inside urban environments with a three-dimensional numerical model. *Environmental Modelling & Software* 13: 373-384. URL: [https://doi.org/10.1016/S1364-8152\(98\)00042-5](https://doi.org/10.1016/S1364-8152(98)00042-5), (accessed: 2020/03/27).
- Bruse, M. (2004): ENVI-met 3.0: Updated Model Overview. 12. URL: <http://envi-met.net/documents/papers/overview30.pdf>, (accessed: 2020/03/20).
- Celette, F., Gaudin, R. & Gary, C. (2008): Spatial and temporal changes to the water regime of a Mediterranean vineyard due to the adoption of cover cropping. *European Journal of Agronomy* 29(4): 153-162. DOI: 10.1016/j.eja.2008.04.007.
- Cho, W. J., Kwon, S. & Choi, J. W. (2009): The thermal conductivity for granite with various water contents. *Engineering Geology* 107: 167-171.
- da Rocha Junior, P. R., Bhattarai, R., Alves Fernandes, R. B., Kalita, P. K. & Vaz Andrade, F. (2016): Soil surface roughness under tillage practices and its consequences for water and sediment losses. *Journal of soil science and plant nutrition* 16(4): 1065-1074. DOI: 10.4067/S0718-95162016005000078.
- Davarzani, H., Smits, K., Tolene, R. M. & Illangasekare, T. (2014): Study of the effect of wind speed on evaporation from soil through integrated modeling of the atmospheric boundary layer and shallow subsurface. *Water Resources Research* 50(1): 661-680. DOI: 10.1002/2013WR013952.
- Deilami, K., Kamruzzaman, M. & Liu, Y. (2018): Urban heat island effect: A systematic review of spatio-temporal factors, data, methods, and mitigation measures. *International Journal of Applied Earth Observation and Geoinformation* 67: 30-42. DOI: 10.1016/j.jag.2017.12.009.
- Dhillon, R., Udompetaikul, V., Rojo, F., Roach, J., Upadhyaya, S., Slaughter, D. Lampinen, B. & Shackel, K. (2014): Detection of plant water stress using leaf temperature and microclimatic measurements in almond, walnut, and grape crops. *Transactions of the ASABE (American Society of Agricultural and Biological Engineers)* 57(1): 297-304. DOI: 10.13031/trans.57.10319.
- Dobos, E. (2011): Albedo. In: Lal, R. (ed.): *Encyclopedia of Soil Science*. Taylor & Francis.
- DWD (Deutscher Wetterdienst) (2020): Climate Data Center. URL: <https://cdc.dwd.de/portal/>, (accessed: 2020/03/31).
- DWI (Deutsches Weininstitut) (2020): Sachsen. URL: <https://www.germanwines.de/tourism/wine-growing-regions/sachsen/>, (accessed: 2020/03/27).
- Engineering ToolBox (2003a): Density of Selected Solids. URL: https://www.engineeringtoolbox.com/density-solids-d_1265.html, (accessed: 2020/03/20).
- Engineering ToolBox (2003b): Emissivity Coefficients Materials. URL: https://www.engineeringtoolbox.com/emissivity-coefficients-d_447.html, (accessed: 2020/03/20).
- Engineering ToolBox (2003c): Specific Heat of some common Substances. URL: https://www.engineeringtoolbox.com/specific-heat-capacity-d_391.html, (accessed: 2020/03/20).
- Fletcher, A., Sinclair, T. & Allen, L. (2007): Transpiration responses to vapor pressure deficit in well watered 'slow-wilting' and commercial soybean. *Environmental and Experimental Botany* 61: 145-151. DOI: 10.1016/j.envexpbot.2007.05.004.
- Flexas, J., Galmés, J., Gallé, A., Gulías, J., Pou, A., Ribas-Carbo, M., Tomàs, M., & Medrano, H. (2010): Improving water use efficiency in grapevines: Potential physiological targets for biotechnological improvement. *Australian Journal of Grape and Wine Research* 16(s1): 106-121. URL: <https://doi.org/10.1111/j.1755-0238.2009.00057.x>.
- Fraga, H., Santos, J.A., Moutinho-Pereira, J., Carlos, C., Silvestre, J., Eiras-Dias, J., Mota, T. & Malheiro, A.C. (2015): Statistical modelling of grapevine phenology in Portuguese wine regions: observed trends and climate change projections. *Journal of Agricultural Science* 154: 795-811. DOI:10.1017/S0021859615000933.
- Fuentes, S., Poblete-Echeverría, C., Ortega-Farías, S., Tyerman, S. & Bei, R.D. (2014): Automated estimation of leaf area index from grapevine canopies using cover photography, video and computational analysis methods. *Australian Journal of Grape and Wine Research* 20(3): 465-473. DOI: 10.1111/ajgw.12098.
- Gattullo, C.E., Mezzapesa, G.N., Stellacci, A.M., Ferrara, G., Occhiogrosso, G., Petrelli, G., Castellini, M. & Spagnuolo, M. (2020): Cover crop for a sustainable viticulture: Effects on soil properties and table grape production. *Agronomy* 10: 1334. DOI: 10.3390/agronomy10091334.
- Geoportal Sachsen (2016a): Downloadbereich DGM1—Sachsen.de. URL: <http://www.geodaten.sachsen.de/downloadbereich-dgm1-4166.html> (accessed: 2020/03/19).
- Geoportal Sachsen (2016b): Downloadbereich DOP -sachsen.de.

- URL: <http://www.geodaten.sachsen.de/downloadbereich-dop-4158.html>. (accessed: 2020/03/19).
- Greer, D.H. (2012): Modelling leaf photosynthetic and transpiration temperature-dependent responses in *Vitis vinifera* cv. Semillon grapevines growing in hot, irrigated vineyard conditions. AoB PLANTS 2012. DOI: 10.1093/aobpla/pls009.
- Grifoni, D., Carreras, G., Zipoli, G., Sabatini, F., Dalla Marta, A. & Orlandini, S. (2008): Row orientation effect on UV-B, UV-A and PAR solar irradiation components in vineyards at Tuscany, Italy. International Journal of Biometeorology 52(8): 755-763. DOI: 10.1007/s00484-008-0168-1.
- Guzmán, G., Cabezas, J. M., Sánchez-Cuesta, R., Lora, Á., Bauer, T., Strauss, P., Winter, S., Zaller, J. G. & Gómez, J. A. (2019): A field evaluation of the impact of temporary cover crops on soil properties and vegetation communities in southern Spain vineyards. Agriculture, Ecosystems & Environment 272: 135-145. DOI: 10.1016/j.agee.2018.11.010.
- Hannah, L., Roehranz, P.R., Ikegami, M., Shepard, A.V., Shaw, M.R., Tabor, G., Zhi, L., Marquet, P.A. & Hijmans, R.J. (2013): Climate change, wine, and conservation. Proceedings of the National Academy of Sciences 10(17): 6907-6912.
- Hunter, J.J., Volschenk, C.G. & Zorer, R. (2016): Vineyard row orientation of *Vitis vinifera* L. cv. Shiraz/101-14 Mgt: Climatic profiles and vine physiological status. Agricultural and Forest Meteorology 228-229: 104-119. DOI: 10.1016/j.agrformet.2016.06.013.
- Hunter, J.J.K., Tarricone, L., Volschenk, C., Giacalone, C., Susete Melo, M. & Zorer, R. (2020): Grapevine physiological response to row orientation-induced spatial radiation and microclimate changes. OENO One 54(2): 411-433.
- Huttner, S. & Bruse, M. (2009): Numerical modeling of the urban climate – a preview on ENVI-met 4.0. The seventh International Conference on Urban Climate, 29 June - 3 July 2009, Yokohama, Japan, 4 S.
- Huttner, S., Bruse, M. & Dostal, P. (2008): Using ENVI-met to simulate the impact of global warming on the microclimate in central European cities. Fifth Japanese-German Meeting on Urban Climate, October 2008, pp 307-312.
- Jackson, R.S. (2014): Wine science. Principles and Applications. 4. Auflage, Academic Press, 960 S.
- Jacobs, C.M.J., van den Hurk, B.M.M. & de Bruin, H.A.R. (1996): Stomatal behaviour and photosynthetic rate of unstressed grapevines in semi-arid conditions. Agricultural and Forest Meteorology 80(2): 111-134. DOI: 10.1016/0168-1923(95)02295-3.
- Jiang, Y. & Weng, Q. (2016): Estimation of hourly and daily evapotranspiration and soil moisture using downscaled LST over various urban surfaces. GIScience & Remote Sensing 54: 95-117. DOI: 10.1080/15481603.2016.1258971.
- Jonckheere, I., Fleck, S., Nackaerts, K., Muys, B., Coppin, P., Weiss, M. & Baret, F. (2004): Review of methods for in situ leaf area index determination: Part I. Theories, sensors and hemispherical photography. Agricultural and Forest Meteorology 121(1): 19-35. DOI: 10.1016/j.agrformet.2003.08.027.
- Koverda, P. (2020): The Ultimate Vapor Pressure Deficit (VPD) Guide. URL: <https://pulsegrow.com/blogs/learn/vpd>.
- Kwast, J., Timmermans, W. J., Gieske, A., Su, Z., Oliosio, A., Jia, L., Elbers, J., Karssen, D. & De Jong, S. (2013): Evaluation of the surface energy balance system (SEBS) applied to ASTER imagery with flux-measurements at the SPARC 2004 site (Barrax, Spain). Hydrology and Earth System Sciences. DOI: 10.5194/hess-13-1337-2009.
- Lee, S.-H., Seo, M.-J., Riu, M., Cotta, J. P., Block, D. E., Dokoozlian, N. K. & Ebeler, S. E. (2007): Vine microclimate and norisoprenoid concentration in Cabernet Sauvignon grapes and wines. American Journal of Enology and Viticulture 58(3): 291-301.
- LfULG (Landesamt für Umwelt, Landwirtschaft und Geologie) (Hrsg.) (2017): Sächsische Weinbergsböden. Steckbrief, 4 S. URL: https://www.boden.sachsen.de/download/boden/YYn_Steckbrief.pdf, (accessed: 2020/03/20).
- Lide, D. R. (2005). CRC Handbook of Chemistry and Physics, Internet Version 2005. CRC Press, Boca Raton, FL. URL: <http://www.hbcpnetbase.com>, (accessed: 2020/07/03).
- Marais, J., Hunter, J. J. & Haasbroek, P.D. (1999): Effect of canopy microclimate, season and region on Sauvignon blanc grape composition and wine quality. South African Journal of Enology and Viticulture 20(1): 19-30. DOI: 10.21548/20-1-2223.
- Marais, J., Calitz, F. & Haasbroek, P.D. (2001): Relationship between microclimatic data, aroma component concentrations and wine quality parameters in the prediction of Sauvignon blanc wine quality. South African Journal of Enology and Viticulture 22(1): 22-26. DOI: 10.21548/22-1-2161.
- Monteith, J.L. & Unsworth, M.H. (2013): Principles of environmental physics: Plants, animals, and the atmosphere, 4. Auflage, Elsevier/Academic Press.
- Oguntunde, P.G., Ajayi, A.E. & Giesen, N. van de (2006): Tillage and surface moisture effects on bare-soil albedo of a tropical loamy sand. Soil and Tillage Research 85(1-2): 107-114. DOI: 10.1016/j.still.2004.12.009.
- Oosterhuis, D.M. & Walker, S. (1987): Stomatal resistance measurement as an indicator of water deficit stress in wheat and soybeans. South African Journal of Plant and Soil 4(3): 113-120. DOI: 10.1080/02571862.1987.10634956.
- Peña Quiñones, A.J., Hoogenboom, G., Salazar Gutiérrez, M.R., Stöckle, C. & Keller, M. (2020): Comparison of air temperature measured in a vineyard canopy and at a standard weather station. PLoS ONE 15(6). DOI: 10.1371/journal.pone.0234436.
- Pieri, P. & Gaudillère, J. (2003): Sensitivity to training system parameters and soil surface albedo of solar radiation intercepted by vine rows. Vitis 42(2): 77-82.
- Pienaar, J. W. (2005): The effect of wind on the performance of the grapevine. URL: <http://hdl.handle.net/10019.1/50486> (accessed 2020/03/22).
- Qin, Z. & Karnieli, A. (1999): Progress in the remote sensing of land surface temperature and ground emissivity using NOAA-AVHRR data. International Journal of Remote Sensing 20(12): 2367-2393; DOI: 10.1080/014311699212074.
- Santos, J.A., Fraga, H., Malheiro, A.C., Moutinho-Pereira, J., Dinis, L.-T., Correia, C., Moriondo, M., Leolini, L., Dibari, C., Costafreda-Aumedes, S., Kartschall, T., Menz, C., Molitor, D., Junk, J., Beyer, M. & Schultz, H.R. (2020): A Review of the Potential Climate Change Impacts and Adaptation Options for European Viticulture. Applied Sciences 10: 3092. DOI:10.3390/app10093092.

- Schwarz, M. (2020): Weingut Martin Schwarz Meißen/Sachsen. URL: <https://www.schwarz-wein.de> (accessed 2020/03/19).
- Sharifi, M., Carter, K., Baker, S., Verhallen, A. & Nemeth, D. (2018): Cover crops effects on grape yield and yield quality, and soil nitrate concentration in three vineyards in Ontario, Canada. *Acta Horticulturae* 1217: 247–256. DOI: 10.17660/ActaHortic.2018.1217.31.
- Steenwerth, K. & Belina, K. M. (2008): Cover crops and cultivation: Impacts on soil N dynamics and microbiological function in a Mediterranean vineyard agroecosystem. *Applied Soil Ecology* 40(2): 370–380; DOI: 10.1016/j.apsoil.2008.06.004.
- Stoutjesdijk, P. & Barkman, J.J. (2014): *Microclimate, Vegetation & Fauna*. BRILL.
- Synnefa, A., Karlessi, T., Gaitani, N., Santamouris, M. & Papakatsikas, C. (2009): Measurement of optical properties and thermal performance of coloured thin layer asphalt samples and evaluation of their impact on the urban environment. *Tagungsbeitrag 2nd International Conference on Countermeasures to Urban Heat Islands*. September 19-23, 2009.
- Valsson, S. & Bharat, A. (2011). Impact of Air Temperature on relative humidity. *Architecture, Time, space and people* 9(2): 20-25.
- Vukicevich, E., Lowery, D. T., Úrbez-Torres, J. R., Bowen, P. & Hart, M. (2018): Groundcover management changes grapevine root fungal communities and plant-soil feedback. *Plant and Soil* 424(1-2): 419–433. DOI: 10.1007/s11104-017-3532-2.
- Weber, B. (1997, unpubl.): *Zur Vegetation auf brachgefallenen Weinbergen im Oberen Elbtal*. Diploma thesis, Martin-Luther Universität Halle-Wittenberg, Halle an der Saale.
- Weinbauverband Sachsen e. V. (2018): *Weinland Sachsen*. Broschüre, 41 S.
- Zeiger, E., Farquhar, G.D. & Cowan, I. R. (Hrsg.) (1987): *Stomatal function*. Stanford University Press.
- Zöphel, B. & Mahn, E.-G. (2000): *Vegetation und Vegetationsentwicklung auf Weinbergsbrachen im Oberen Elbtal (Freistaat Sachsen)*. *Hercynia N.F.* 33: 63- 98.

Addresses of the Authors:

Noirault, Adrien*: ENS de Lyon, Biology department, 69342, Lyon, France, e-mail: adrien.noirault@ens-lyon.fr

Achtziger, Roland; Richert, Elke: TU Bergakademie Freiberg, Institut für Biowissenschaften / Interdisziplinäres Ökologisches Zentrum (IÖZ), AG Biologie / Ökologie, Leipziger Straße 29, 09599 Freiberg; E-Mail: roland.achtziger@ioez.tu-freiberg.de; elke.richert@ioez.tu-freiberg.de

Goldberg, Valeri: TU Dresden, Institut für Hydrologie und Meteorologie, Professur Meteorologie, Piennner Str. 23, 01737 Tharandt, E-Mail: valeri.goldberg@tu-dresden.de

Köstner, Barbara: LandCARE gGmbH, Zwickauer Straße 137, 01187 Dresden, E-Mail: info@landcare-ggmbh.de

*Corresponding author